Photoassisted sequential resonant tunneling through superlattices.

Jesús Iñarrea and Gloria Platero
Instituto de Ciencia de Materiales (CSIC) and Departamento de Fisica de la Materia Condensada C-III, Universidad Autonoma, Cantoblanco, 28049 Madrid, Spain.

arXiv:cond-mat/9506103v1 22 Jun 1995

We have analyzed theoretically the photoassisted tunneling current through a superlattice in the presence of an AC potential. For that purpose we have developed a new model to calculate the sequential resonant current through a superlattice based in the Transfer Hamiltonian method. The tunneling current presents new features due to new effective tunneling channels coming from the photoside bands induced by the AC field. Our theoretical results are in good agreement with the available experimental evidence.

73.40.G

The analysis of resonant tunneling through semiconductor superlattices (SL) has a lot of interest from a fundamental point of view as well as for its applications as microelectronic devices. Their transport properties were first investigated in 1970 by Tsu and Esaki [1]. Later, (1971), Kazarinov and Suris [2] studied theoretically the current-voltage curve for a SL and predicted the existence of peaks corresponding to sequential resonant tunneling between adjacent wells depending on the coupling between the quantum wells. In 1973 Tsu and Esaki [3] presented a calculation on resonant tunneling through multiple barriers, and in 1974 Esaki and Chang [4]observed oscillatory conductance in a SL heterostructure. Since then, the transport properties of those structures have been under intense experimental [5] and theoretical [6] investigation, not only under static but also at high frequency fields.
When a static electric field is applied to a SL the overlap of wave functions between wells decreases and as a result the miniband tends to split into a series of states which are distributed sequentially along the field direction. In other words, a ladder of states, or Stark ladder is formed. For high static fields at which the voltage drop over one period is large compared with the miniband width, coupling is completely destroyed and the SL effectively becomes a series of isolated quantum wells. Under these conditions, the current-voltage characteristic has the form of a set of narrow peaks corresponding to the tunneling of an electron from the ground state in one cell to an excited state in a neighboring cell (see fig. 1.a). In reality each peak is broadened because tunneling is even possible out of resonance due to scattering with phonons, surface roughness etc. As a result the current-voltage curve has a finite current between peaks rather than zero current [7,8].

In this paper we analyze the photoassisted sequential resonant tunneling current through a SL in the presence of an AC potential. The AC field induces absorption and emission processes which are reflected as new features in the current density. These new features in the tunneling current are due to new effective tunneling channels coming from the photoside bands (see fig. 1.b), which are opened and which produce additional current steps in the characteristic current-voltage curve.
In order to study the sequential resonant tunneling through a SL, before applying the AC field, we have developed a model in the framework of the Transfer Hamiltonian formalism [9] to calculate the current through the SL, considering a uniform static electric field along the structure. In this model we have calculated first the probability for the electrons to cross each individual barrier from one well to the adjacent one, and from that the density current. The total current is obtained when all the individual currents result to be equal. Under this condiction we obtain also that all the Fermi levels in the different wells are equal (we are considering uniform static electric field along the SL and neglected the electron-electron interaction effects). The expression we obtain for the total current can be written as:

$$J_T = \frac{e\hbar}{2\pi m^*}\frac{k_1(E_{11})k_2(E_{11})T_s(E_{11})}{\alpha_{12}(E_{11})\alpha_{23}(E_{11})} \times \left[L(E_{22}-E_{11})+L(E_{23}-E_{11})\right]E_1 \qquad (1)$$

where $\alpha_{ij} = (w_b + 1/\alpha_i + 1/\alpha_j)$, being α_i (α_j) the perpendicular electronic wave vector in the barriers i and j and w_b is the barrier width. $T_s(E_{11})$ is the single barrier transmission coefficient, $k_1(E_{11})$ and $k_2(E_{11})$ are the perpendicular component of the electronic wave vector in the first and second well respectively, all of then evaluated at the energy of the ground (first) state in the first well ((E_{11})). E_{ij} represents the energy corresponding to the i well and j state referred to the conduction band bottom in the emitter. $L(E_{2(2,3)}-E_{11}) = \frac{\gamma}{(E_{2(2,3)}-E_{11})^2+\gamma^2}$ where γ is the half width of the well state. Finally E_1 represents the Fermi level for the wells and corresponds to a bidimensional electron density.

The carrier charge density in the wells in a SL can be obtained by two ways: from the emitter which is considered to be heavily doped or from photoinjection from the valence band. Our model can be adapted in any of the two situations. All the scattering processes which are responsible for the tunneling out of resonance are taken into account in our model, through a finite broadening in the well states which is represented by the Lorentzian function $L(E_{2(2,3)} - E_{11})$. We have applied this model to analyze the tunneling current through a SL formed by 50 periods of a GaAs well with 13.3 nm width and an AlAs barrier with 2.7 nm width. The wells are not doped and the carriers are provided by photoinjection from the valence band in order to keep constant in average the number of electrons resposible for the current at every external dc bias. The results are shown in figure 2 where we can see the two main peaks corresponding to the sequential resonant tunneling from the ground state of one well to the first and second excited states of the adjacent one. It can be observed how these peaks are broadened and a finite current different from zero between peaks which is due to the

different scattering processes that take place during the tunneling from one well to the next one as we have explained above. The general aspect of the current-voltage curve agrees with the physics of the sequential resonant tunneling when the dc electric field is dropped uniformly across the sample and is qualitatively similar to the ones obtained in the available experiments [7,8]. The time which describes the relaxation between the states involved in the resonant tunneling process due to momentum relaxing collision is about $10^{-13}s$. [4,7]. With this time we estimate a half width for the broadening corresponding to the well states of $\gamma = 5 - 10meV$. For the curve in figure 2 we have used a value of $\gamma = 10meV$.

Once we have developed a model to obtain the current through a SL, we have analyzed theoretically the effect of an external AC field on the sequential resonant tunneling of a SL. We have used again the Transfer Hamiltonian formalism to obtain the probability for an electron to cross from one well to the next one ($i \rightarrow j$) in the presence of a time oscillating field (both wells are oscillating):

$$P_{ij} = \lim_{\alpha \to 0} \frac{d}{dt} \left| \frac{1}{i\hbar} \int_{-\infty}^{t} < \Psi_{j2}|V_L|\Psi_{i1} > e^{\alpha t'} dt' \right|^2 \qquad (2)$$

where V_L represents the potential barrier. Ψ_{in} are the resulting electronic wave functions in the time modulated quantum well, i.e, for a Hamiltonian of the form $H = H_0 + eFzcoswt$ being F the intensity for the AC electric field, w its frequency, the subscript i represents the well and n represents the resonant states. Those electronic wave functions can be written following Tien and Gordon [10]:

$$\Psi_{in} = \Psi_0 \sum_{-\infty}^{\infty} J_n(\beta_i) e^{-inwt} \qquad (3)$$

where Ψ_0 is the unperturbed wave function (without the AC field) , $J_n(\beta)$ are the Bessel function of the first kind, and $\beta_i = eFz_i/\hbar w$, being z the spatial coordinate in the SL axis. We consider that the AC field affects the whole structure increasing uniformly from the emitter, which is considered to be fixed, to the collector which is affected by the field with its total amplitude. In between, all the wells are oscillating with increasing intensity depending on its spatial coordinate. From the probability we can calculate the current through each individual barrier inside the SL. We obtain the total current when all the individual currents result to be equal in the same way as we have explained above. Finally we have an expression for the total current which is crossing the SL in the presence of an external AC field:

$$J_T = \frac{e\hbar}{2\pi m^*} \frac{k_1(E_{11})k_2(E_{11})T_s(E_{11})}{\alpha_{12}(E_{11})\alpha_{23}(E_{11})} E_1 \times \sum_{m,n=-\infty}^{\infty} J_m^2(\beta_2) J_n^2(\beta_1) \times [L(E_{22} - E_{11} + (m-n)\hbar w) + (E_{23} - E_{11} + (m-n)\hbar w)] \qquad (4)$$

where $\beta_{2,1} = \frac{eFz_{2,1}}{\hbar w}$ being $z_{2,1}$ the spatial coordinates corresponding to the center of the second and first wells respectively.

We have applied the model described above to the available experimental evidence [11]. We have calculated the current through a SL consisting of 100 periods of 33 nm $GaAs$ wide quantum wells separated by 4 nm $Al_{0.3}Ga_{0.7}As$ barriers. As in the paper [11], we consider the radiation is coupled into the sample by using an antenna and produce an electric field intensity of several kV/cm . In fact we have use an electric field intensity of $10^5 V/m$ and a frequency of $2.11 \times 10^{12} s^{-1}$ which is equivalent to a photon energy of $\hbar w = 1.39meV$. As in the case without AC field, we have considered a bidimensional density for the electrons in the wells of the order of $E_1 = 10^{11} cm^{-2}$ and a half width for the resonant state of the order of $5meV$. In figure 3 we present the results obtained for the current density versus the dc voltage for the parameters described above. Continuous line corresponds to no AC field present and dotted line to the AC field present. Figure 3a presents the results involving the first resonant condition or in other words, the first peak corresponding to the tunneling from the ground state of one well to the first excited state of the next one. In figure 3b we can see an extended view which includes also the second peak corresponding to the tunneling to the second excited state. Under an AC field new steps appear in the current-voltage curve(dotted line) and can be observed how the main current peaks decrease in intensity referred to the case of no AC field present. All these new features can be explained in terms of photon assisted tunneling. The presence of the AC field produce new channels for the tunneling coming from the photoside bands induced by the time dependent field and because of that electrons in the ground state of one well can tunnel to the excited states of the adjacent well with the absorption or emission of one or more photons. Or in other words, the tunneling process now, can take place between the ground state of one well and a photoside band in the adjacent well (see fig. 1.b). This is the reason for the positive structure in the bias regions around the main current peaks and also for the smaller intensities of those peaks since the electron density in the tunneling has to be conserved for both cases, with or without AC field. All these new features that can be seen in the current-voltage curve are in good agreement with the results obtained in the available experimental evidence [11]. According to all the explained above, the new effective tunneling channels due to the photoside bands are predicted to appear at energies of $\pm n\hbar w$ from the resonant states. However these channels are not reflected individually in the current-voltage curves, where a continuous positive plateau appear at both sides of the main central peak. This is not observed either in the experimental results [11]. We think this is due to the small AC field frequency we are using ($1.39meV$), compared to the half width of the well resonant state ($5meV$). If we want to see the different channels contributions individually in the current-voltage curve, we have to change the parameters, making the AC field frequency bigger compared to the half width of the state. Using our model we have calculated the current density for the same SL as before and in the presence of an AC field with the an intensity of $F = 1.510^5 V/m$ and with a frequency of $\hbar w = 5meV$. The other different parameter has been the half width for the resonant state which now is of the order of $\gamma = 1meV$. The results are shown in figure 4.a, where we can see very clearly the individual contributions corresponding to the new effective tunneling channels of $\pm 2\hbar w$, $\pm 1\hbar w$ and for the two main resonant peaks. In figure 4.b we compared the

results for the AC field present (dotted line) versus the case with no time dependent field present (single line). Is interesting to note in figure 4, how the steps and plateaus from figure 3, become real current peaks which agrees with the concept of photoside bands that produce new effective tunneling channels. For those new peaks, the tunneling take place from the ground state of one cell to a photoside band of the next cell. In conclusion, the effect of an AC field on the tunneling current density through a SL has been analyzed. A new theoretical model ,based in the Transfer Hamiltonian method, to calculate the current in SL has been presented and has been generalized to the case of a time dependent field present. The effect of the AC field on the current density is a new tunneling mechanism which still is resonant and sequential but based in photon side bands induced but the presence of the time dependent field. New features for the current have been obtained: positive steps and plateaus that can become real current peaks with the appropriate conditions. Our results are in good agreement with the available experimental evidence. Our model can be improved taken into account the effect of the charge inside the well on the SL potential profile which induces the oscillatory dependence of the current with the applied static voltage due to the formation of domains in the SL. This is the aim of a future work.

This work has been supported by the Comision Interministerial de Ciencia y Tecnologia of Spain under contract MAT 94-0982-c02-02 , by the Comission of the European Communities under contract SSC-CT 90 0201 and by the Acción Integrada Hispano-Alemana 84-B.

FIG. 1. a) Schematic diagram of sequential resonant tunneling of electrons through a superlattice. The potential energy drop across a superlattice period is equal to the energy difference between the ground state and the first excited state. b) Sequential resonant tunneling in the presence of an AC field. Tunneling can be produced through new effective channels induced by the time dependent field.

FIG. 2. Current density versus voltage for sequential resonant tunneling through a superlattice of 50 periods of 2.7 nm of AlAs barrier and 13.3 nm of GaAs well The half width of the resonant state is of $10meV$.

FIG. 3. a) Current density versus voltage for sequential resonant tunneling through a SL with the parameters of [11], and a half width of $5meV$, in the presence of an AC field with an intensity $10^5V/m$ and a frequency of $1.39meV$ (dotted line) and with no AC. field present (continuous line). b) Same as in a) for an extended view of the applied voltage.

FIG. 4. a) Current density versus voltage for sequential resonant tunneling through a SL with the parameters of [11], and a half width of $1meV$, in the presence of an AC field with an intensity $1.5x10^5V/m$ and a frequency of $5meV$. b) Same as in a) for (dotted line) AC present and (continuous line) without AC applied to the sample.

[1] L.Esaki and R.Tsu. IBM, J.Res.Dev.**14**, 61 (1970).

[2] R.F.Kazarinov and R.A.Suris, Fiz.Tech.Poluprovodn. **6** 148 (1972). [Sov. Phys. Semicond. **6** 120 (1972).]

[3] R.Tsu and L.Esaki, Appl. Phys. Lett. **22** 562 (1973).

[4] L.Esaki and L.L.Chang. Phys. Rev. Lett. **330** 495 (1974).

[5] T.C.L.G.Sollner, W.D.Goodhue, P.E.Tannenwald, C.D.Parker and D.D.Peck, Appl. Phys. Lett. **43** 588 (1983). E.E.Mendez, W.I.Wanf, B.Ricco and L.Eski, Appl. Phys. Lett.**47** 415 (1985).

[6] B.Ricco and M. Ya Azbel. Phys Rev. B **29** 1970 (1984). S.Luryi, Appl.Phys.Lett. **47** 490 (1985).

[7] F.Capasso, K. Mohammed and Alfred Y.Cho. Appl. Phys. Lett. **48** 478 (1986).

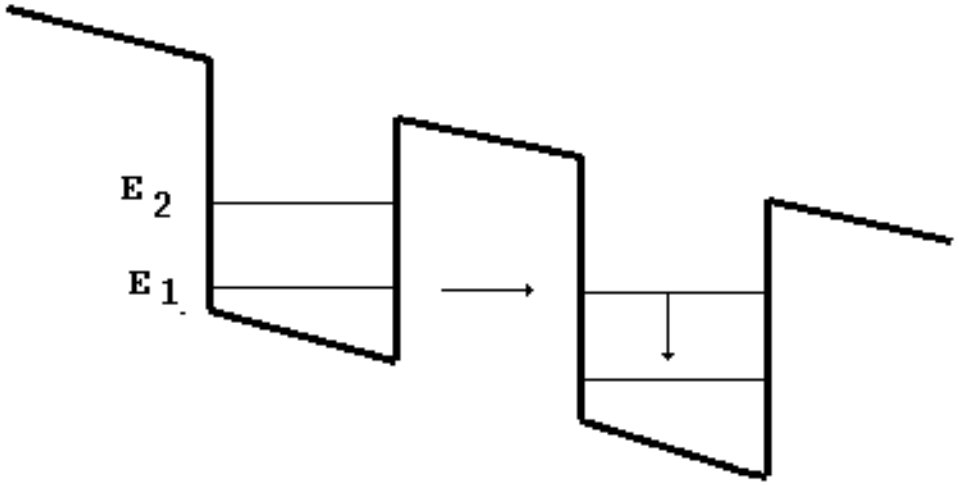
[8] The Physics of Instabilities in Solid Sates Electron Devices. M.P.Shaw, V.V.Mitin, E.Scholl and H.L.Grubin. Plenum Press, New York (1992). p. 147.

[9] J.Bardeen, Phys.Rev.Lett. **6** 57 (1961).

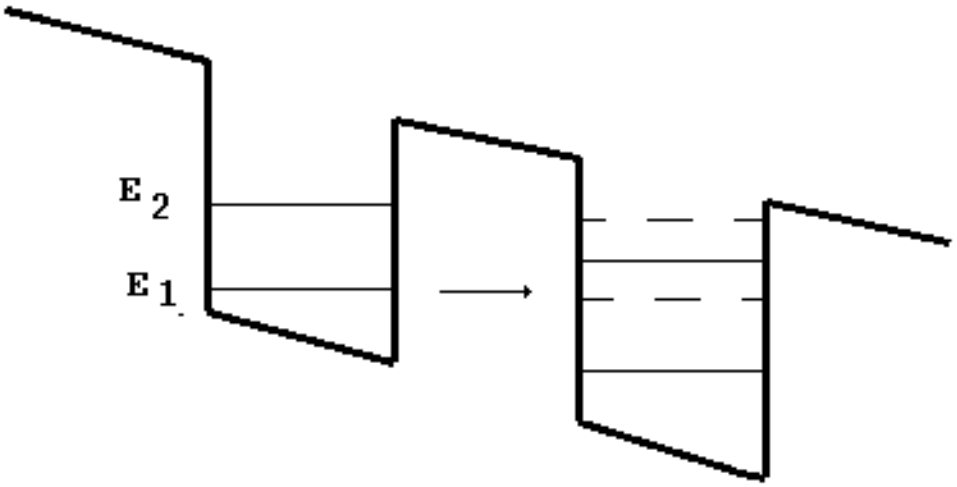
[10] P.K.Tien and J.P.Gordon, Phys.Rev. **129** 647 (1963).

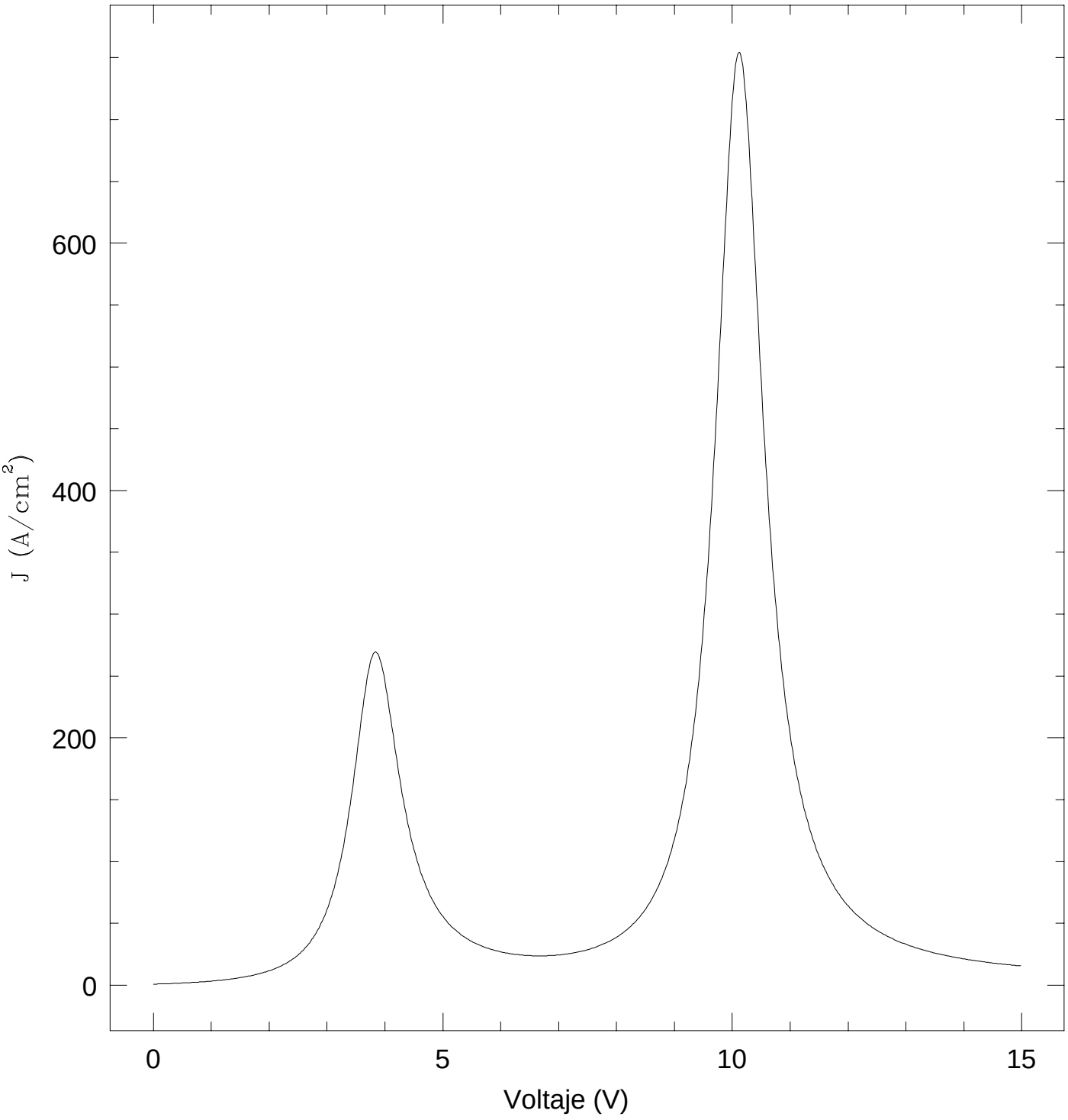
[11] P.S.S.Guimaraes, Brian J.Keay, Jann P.Kaminsky, S.J.Allen, P.F.Hopkins, A.C.Gossard, L.T.Florez and J.P.Harbison. Phys.Rev.Lett **70** 3792 (1993).

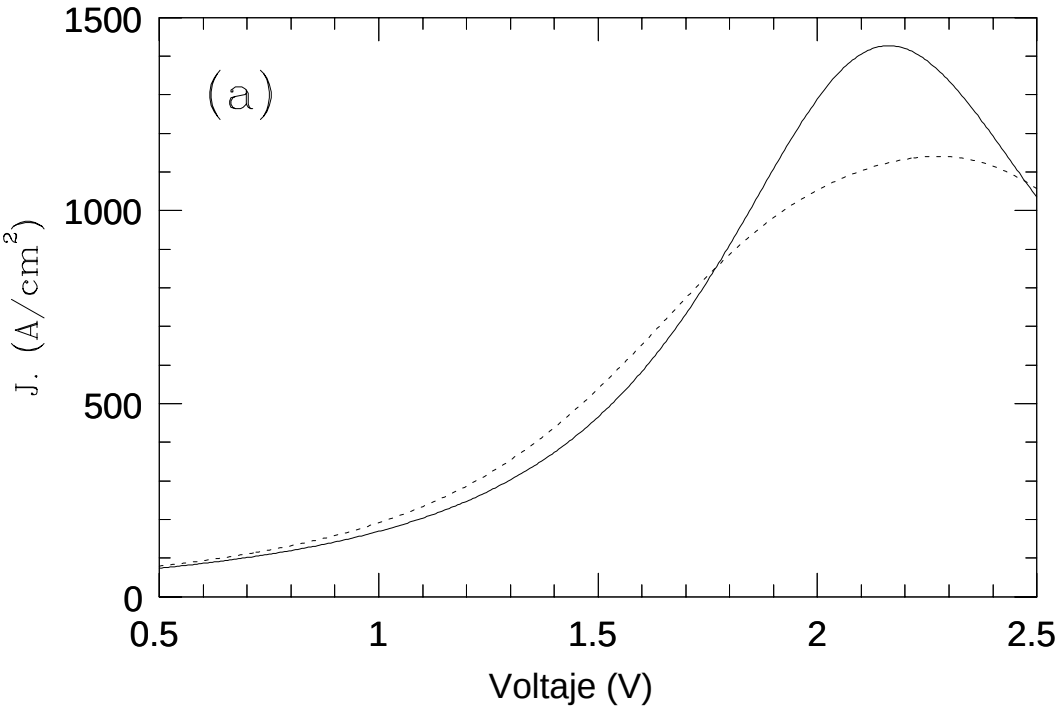
a)

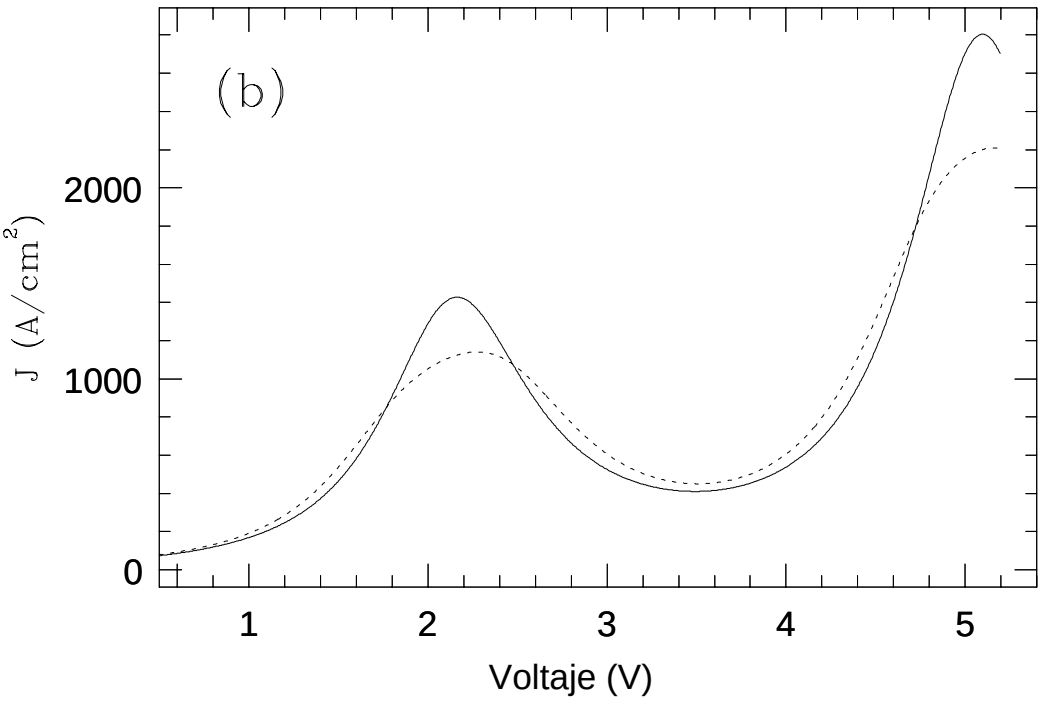


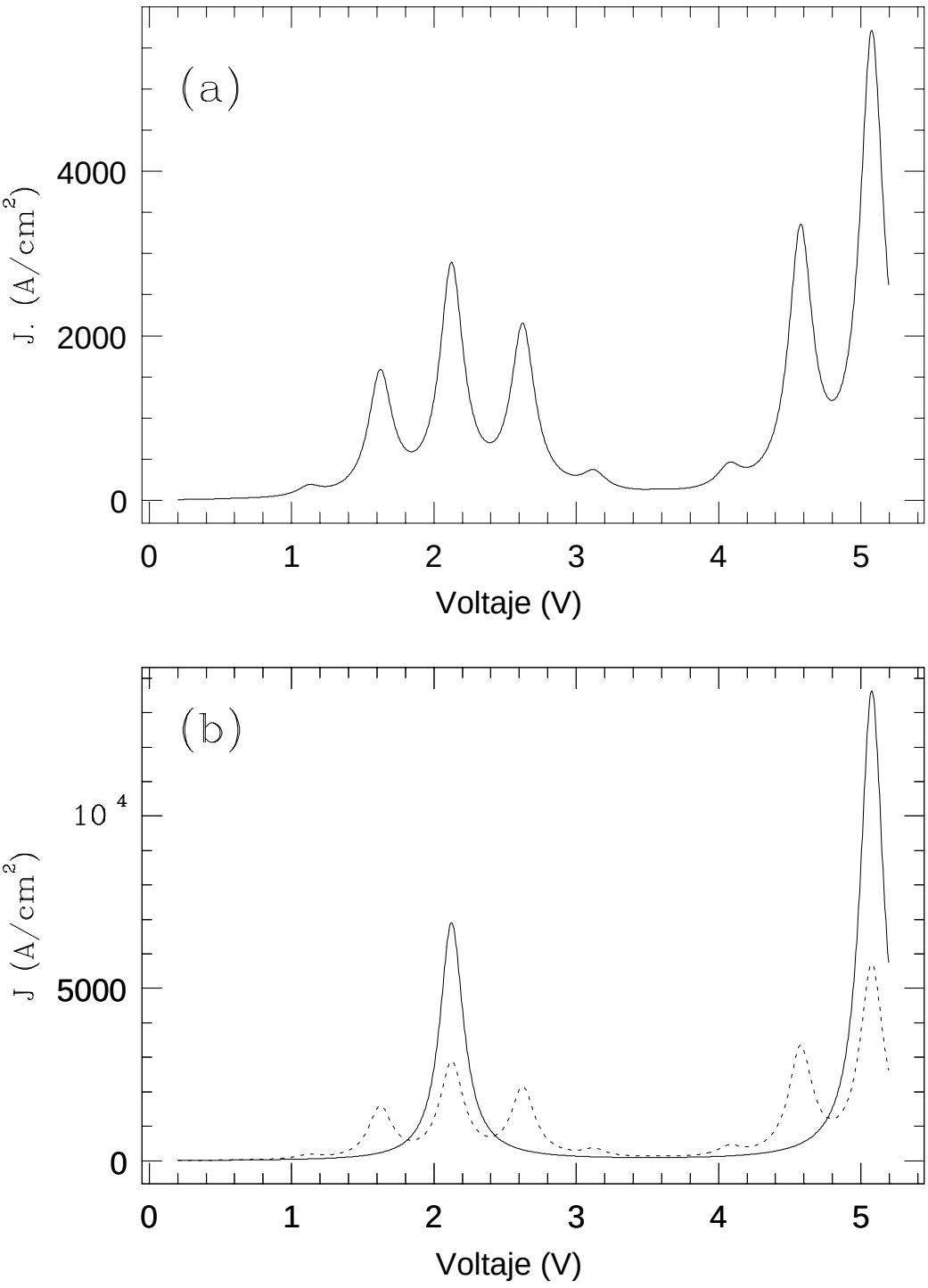
b)




600
400
200
0
J (A/cm^2)
0
5
10
15
Voltaje (V)


(a)
1500
1000
500
0
J. (A/cm^2)
0.5
1
1.5
2
2.5
Voltaje (V)


(b)
2000
1000
0
J (A/cm^2)
1
2
3
4
5
Voltaje (V)


(a)
J. (A/cm^2)
4000
2000
0
0
1
2
3
4
5
Voltaje (V)
(b)
J (A/cm^2)
10^4
5000
0
0
1
2
3
4
5
Voltaje (V)